



ELSEVIER

Journal of Magnetism and Magnetic Materials 169 (1997) 261–270

**J**ournal of  
**M**agnetism  
**and**  
**M**magnetic  
**materials**

# Superparamagnetic behavior of Fe<sub>3</sub>GaAs precipitates in GaAs

T.M. Pekarek<sup>a,\*</sup>, B.C. Crooker<sup>b</sup>, D.D. Nolte<sup>a,c</sup>, J. Deak<sup>a,c</sup>, M. McElfresh<sup>a,c</sup>,  
J.C.P. Chang<sup>c,d</sup>, E.S. Harmon<sup>c,d</sup>, M.R. Melloch<sup>c,d</sup>, J.M. Woodall<sup>c,d</sup>

<sup>a</sup>Department of Physics, Purdue University, West Lafayette, IN 47907, USA

<sup>b</sup>Department of Physics, Fordham University, Bronx, NY 10458, USA

<sup>c</sup>MRSEC for Technology-Enabling Heterostructure Materials, Purdue University, West Lafayette, IN 47907, USA

<sup>d</sup>School of Electrical Engineering Purdue University, West Lafayette, IN 47907, USA

Received 12 February 1996; revised 6 December 1996

## Abstract

We present magnetization measurements on Fe<sub>3</sub>GaAs clusters distributed throughout a layer 170 nm thick at the surface of a GaAs wafer. The clusters have 1.5, 4.4, and 28 nm mean diameters and effective moments of 240, 6000, and 10 000 Bohr magnetons. The 1.5 and 4.4 nm mean diameter clusters are internally aligned ferromagnetically and exhibit superparamagnetic behavior with low saturation fields and well-defined blocking temperatures. Superparamagnetic fits to the field-dependent magnetization well above the blocking temperature indicate a particle size distribution in agreement with electron microscopy studies. We find evidence in the 28 nm mean diameter clusters for multiple domains. Zero-field-cooled and field-cooled measurements reveal blocking temperatures of approximately 3.8, 35, and 290 K for increasing cluster diameters.

PACS: 75.50.Pp; 75.60.Jp; 61.70.Tm

Keywords: Superparamagnetism; granular semiconductor; Fe<sub>3</sub>GaAs; Transition-metal implanted GaAs; Magnetic semiconductor

## 1. Introduction

Composite materials consisting of GaAs containing clusters of Fe<sub>3</sub>GaAs are the semiconductor ana-

logs of granular metallic systems such as Co–Cu, Fe–Cu, and Co–Ag [1–7]. A key feature of the latter systems is the superparamagnetic response of the clusters leading to giant magnetoresistance (GMR) with potential uses such as magnetic recording heads or field-actuator devices. Giant magnetoresistance was first observed in multilayer systems [8] and has resulted in an extensive

\* Corresponding author. Tel: +1 765 494 5513; fax: +1 765 494 0706; e-mail: pekarek@physics.purdue.edu.

literature [9–16]. The maximum change in resistance observed in these materials surpasses the traditional magnetoresistive materials such as Permalloy. Recently, GMR was observed in a non-multilayer magnetic system by Berkowitz and coworkers [17] and Xiao and coworkers [18, 19]. The superparamagnetic response of these granular metallic systems is key to the observed GMR. There is a distinct advantage in obtaining GMR in a semiconducting system similar to the metallic systems because it can be directly integrated on a wafer with other semiconductor components such as field-effect transistor amplifiers. Additionally, semiconducting systems offer carrier density and type (electrons or holes) as added design variables.

In addition to the potential for GMR in these materials, the  $\text{Fe}_3\text{GaAs}$  precipitates are metallic. This may lead to better performance characteristics for opto-electronic applications than those observed for the previously studied semimetallic As clusters [20–24]. The existence of a GMR material that also has interesting optical properties could give rise to useful magneto-optic applications [17–23].

It has been previously shown that  $\text{Fe}_3\text{GaAs}$  precipitates can be fabricated in GaAs [24]. Also, early work on iron-doped GaAs showed a Curie-like behavior for bulk samples [25, 26]. But, the magnetic behavior of the nanocrystalites in a GaAs host remained undetermined. Related systems such as  $\text{In}_{1-x}\text{Mn}_x\text{As}$  and MnGa films have also been studied [27–29]. However, neither system exhibits superparamagnetism. Another related system based on manganese-doped GaAs which is a magneto-optic material has been shown to form slightly larger precipitates primarily on the surface of GaAs [30, 31]. These precipitates were found to contain multiple domains and exhibited hysteresis.

In this paper we report on the magnetic properties of metallic  $\text{Fe}_3\text{GaAs}$  precipitates located in a layer within 170 nm of the surface of a GaAs wafer. The key feature of this system is the superparamagnetic behavior of the  $\text{Fe}_3\text{GaAs}$  precipitates. We also present measurements of cluster blocking transitions for samples with different cluster sizes which can be explained by the dipolar interaction between clusters.

## 2. Experimental details

Samples containing  $\text{Fe}_3\text{GaAs}$  clusters were fabricated from commercial semi-insulating GaAs wafers. Iron was ion implanted at room temperature to a concentration of  $1 \times 10^{16}$  ions/cm<sup>2</sup> using an energy of 170 keV. Rapid thermal annealing of samples at 950°C for 30 s or at 675°C for 30 min resulted in metallic  $\text{Fe}_3\text{GaAs}$  precipitates. Increasing the temperature and duration of the anneals yields larger cluster sizes consistent with Ostwald ripening theory [32]. Additionally, we studied an unannealed sample which was stored at room temperature for several months before magnetic measurements were conducted. Transmission electron microscopy (TEM) studies have been conducted on all three samples and are discussed below; TEM results for the 950°C annealed sample have been reported previously [24].

For the magnetic measurements the samples were thinned to  $\sim 50$   $\mu\text{m}$  and measured in a Cryogenic Consultants Limited (CCL) SQUID magnetometer. Measurements were taken in fields from 0 to 6 T and at temperatures from 1.5 to 324 K. The diamagnetic contribution to the signal was determined at high field where the superparamagnetic signal is nearly saturated and was subtracted from the data to reveal the magnetic behavior of the  $\text{Fe}_3\text{GaAs}$  clusters. The increasing scatter between 0.15 and 0.5 tesla is due to the growth of the diamagnetic signal and due to reduced field stability above 0.15 tesla in our magnetometer.

## 3. Experimental results and discussion

### 3.1. Superparamagnetic behavior

Magnetization versus field measurements on the 675°C annealed sample are shown in Fig. 1. Measurements were taken at 99 and 298 K. The data are reasonably well described by a simple Brillouin function assuming individual particles with a single moment of 6 000 Bohr magnetons, indicating that the Fe moments are aligned ferromagnetically within each  $\text{Fe}_3\text{GaAs}$  particle. The effective moment, equal to the sum of the individual moments of all the iron in a cluster, responds to an

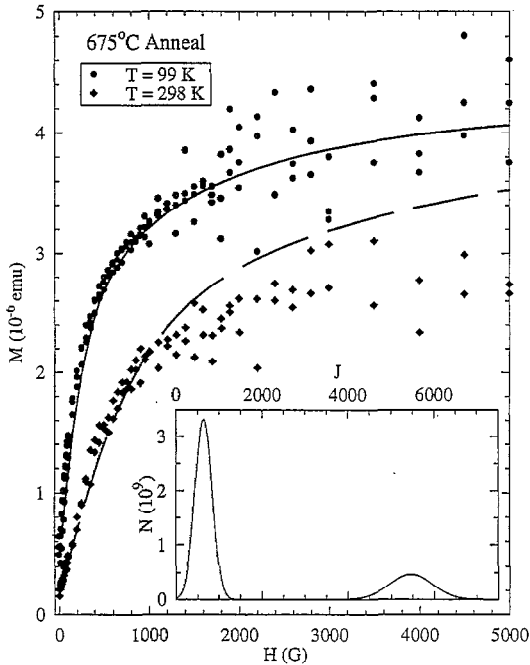


Fig. 1. Magnetization versus field for the 675°C annealed sample at 99 and 298 K. The solid lines are theoretically calculated magnetization curves using the particle size distribution shown in the inset assuming a superparamagnetic response. TEM studies show that the larger cluster population forms at defect sites and on the surface while the smaller cluster population forms in the bulk GaAs. The scatter at high fields is due to the increasing diamagnetic signal.

applied field as a single nearly free spin. This is the hallmark of superparamagnetism comparable to that seen in the granular metallic Co–Cu system. These results are encouraging for potential applications as GMR devices. However, deviations above the Brillouin response at low field and below the Brillouin response at high field suggest the presence of both larger and smaller clusters. Therefore, to obtain a more accurate fit, it was necessary to consider a distribution of cluster sizes.

As the sample is annealed, the precipitates grow with time as the iron migrates to the stable hexagonal  $\text{Fe}_3\text{GaAs}$  structure from a larger and larger volume of Fe-implanted GaAs. As a first approximation, the number of clusters  $N$  with a given size is expected to be Gaussian in the volume from which the iron migrated. This volume is more con-

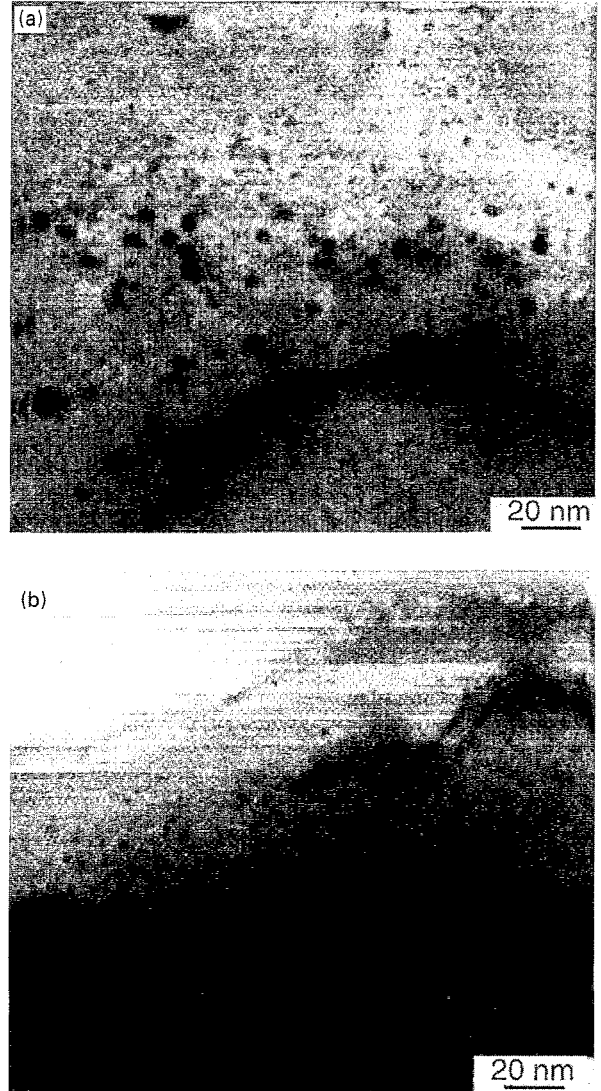


Fig. 2. (a) TEM image of a GaAs sample that was implanted with Fe and annealed for 30 min at 675°C. Precipitates are clearly seen in the bulk GaAs with larger clusters forming at defect sites and on the surface. (b) TEM image of an unannealed GaAs sample that was implanted with Fe. Small precipitates are clearly seen.

veniently expressed in terms of the number of iron atoms or equivalently the total angular momentum  $J$  of the super-paramagnetic clusters.

The TEM data, shown in Fig. 2(a), show a population of smaller clusters 3–5 nm in diameter

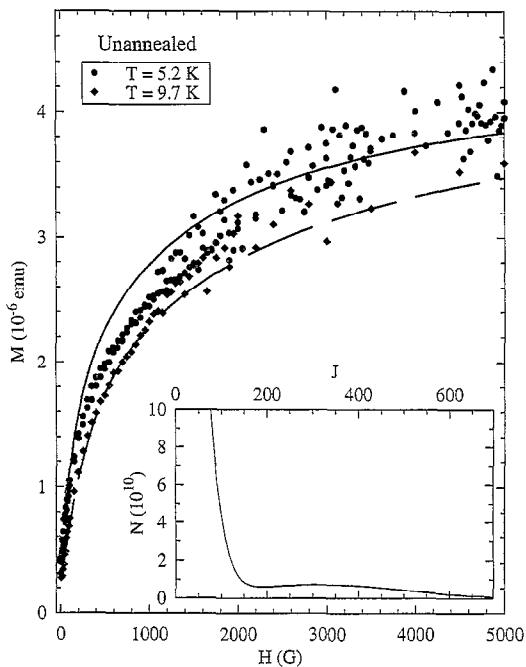


Fig. 3. Magnetization versus field for the unannealed sample at 5.2 and 9.7 K. The solid lines are theoretically calculated magnetization curves using the particle size distribution shown in the inset. The high moment tail in the distribution likely forms at defect sites within the GaAs wafer. The 5.2 K magnetization is suppressed below the free spin model prediction due to the nearby blocking temperature. The scatter at high fields is due to the increasing diamagnetic signal.

distributed in the bulk GaAs and a population of larger clusters up to 20 nm in diameter at line defects and on the surface. We modeled this observed distribution for the 675°C annealed sample as a pair of Gaussians with total angular momentum  $J$  centered at 640 and 5450 as shown in the inset of Fig. 1. The magnetization for this distribution was calculated assuming a superparamagnetic response and is shown as solid lines in Fig. 1. As can be seen, the observed TEM distribution provides a good description of the magnetic behavior in this sample assuming superparamagnetic clusters.

Magnetization versus field measurements on the unannealed sample were taken at 5.2 and 9.7 K (Fig. 3). The key features are the large moment ( $\sim 240$  Bohr magnetons) superparamagnetic be-

havior of the clusters and 75% saturation in a 4000 G field at 9.7 K. The data can be approximately fit with a simple Brillouin function assuming a single 2.0 nm diameter cluster size with a moment of 240 Bohr magnetons. Again, deviations above the Brillouin response at low field and below the Brillouin response at high field suggest the presence of both larger and smaller clusters.

The observed magnetization versus field response of the unannealed sample indicates a substantial population of small superparamagnetic clusters ( $\sim 1.5$  nm) in the bulk GaAs with a tail in the distribution extending up to 5 nm in diameter. We modeled this as a pair of overlapping Gaussian distributions which is shown in the inset of Fig. 3 as a function of  $J$ . The scale has been set to expose the large diameter tail. Shown in Fig. 3 as solid lines are theoretically calculated magnetization curves using the particle size distribution shown in the inset. The 9.7 K fit is in good agreement with the magnetization measurements. The 5.2 K data fall below the predicted values due to the nearby blocking temperature of  $\sim 3.8$  K discussed below. Near this temperature, coupling between individual clusters becomes important leading to a negative non-linear term in the susceptibility [33–35].

TEM measurements have been performed on small portions of the unannealed (Fig. 2(b)) sample. Initially, we had assumed that the unannealed sample would not contain clusters. However, the magnetic data indicates the presence of a distribution of clusters. TEM images of the unannealed sample were taken which confirm that the clusters are in fact present with a distribution in agreement with the magnetization results shown in the inset of Fig. 3. The observation of clusters in this sample indicates either a substantial mobility of the iron at room temperature or a slightly elevated temperature of the sample during the implantation process.

The clusters in the unannealed sample (mean particle diameter 1.5 nm) are significantly smaller than previously observed [24]. This, along with the slightly larger clusters (mean particle diameter 4.4 nm) observed in the 675°C annealed sample, is an important result since it demonstrates the ability to form clusters exhibiting superparamagnetism over a wide range of particle sizes including the

optimum particle sizes of a few nm that was found in the metallic systems [7]. In comparison, the Mn-based system is reported to contain much larger  $\sim 50$ – $100$  nm precipitates which form only on the surface of the GaAs host [31].

It was suggested previously that magnetic measurements on this system would provide further evidence of the structure of the clusters [24]. Selected area diffraction patterns (SADPs) were analyzed along the  $[\bar{2} 3 3]$  and  $[0 1 2]$  poles consistent with either a  $\text{Fe}_3\text{GaAs}$  or  $\text{FeAs}$  structure. However, SADP along the  $[0 1 1]$  direction was found to be inconsistent with the  $\text{FeAs}$  structure. It was suggested that the  $\text{Fe}_3\text{GaAs}$  structure could be further confirmed by magnetic measurements since  $\text{Fe}_3\text{GaAs}$  is ferromagnetically aligned whereas  $\text{FeAs}$  is antiferromagnetic [24, 26]. Our magnetic results on the  $675^\circ\text{C}$  and unannealed samples show clearly that the clusters are internally aligned ferromagnetically, are single domain, and exhibit superparamagnetism. This provides further evidence for the  $\text{Fe}_3\text{GaAs}$  structure of the magnetic precipitates.

Magnetization versus field measurements on the  $950^\circ\text{C}$  annealed sample are shown in Fig. 4. Measurements were taken at 298 K near the blocking temperature and at 99 K. The data can be fit with a Brillouin function assuming a single superparamagnetic cluster size of 7 nm diameter with a moment of 10 000 Bohr magnetons. This value is inconsistent with measurements made by TEM which clearly reveal clusters 20–40 nm in diameter. Particles 20 nm in diameter would be nearly saturated at room temperature in fields of a few gauss, orders of magnitude below the value of  $\sim 2000$  G evident in Fig. 4. Due to the presence of a blocking transition near room temperature, the interactions between clusters are important over the full temperature range accessible to our magnetometer. As discussed above, the magnetization is suppressed below the simple Brillouin function as one approaches the blocking transition. We do not believe, however, that this effect would be large enough to explain the discrepancy between the cluster size obtained from TEM measurements and that obtained in an analysis of the magnetic data.

A second possibility is the presence of multiple domains in these clusters which becomes a concern

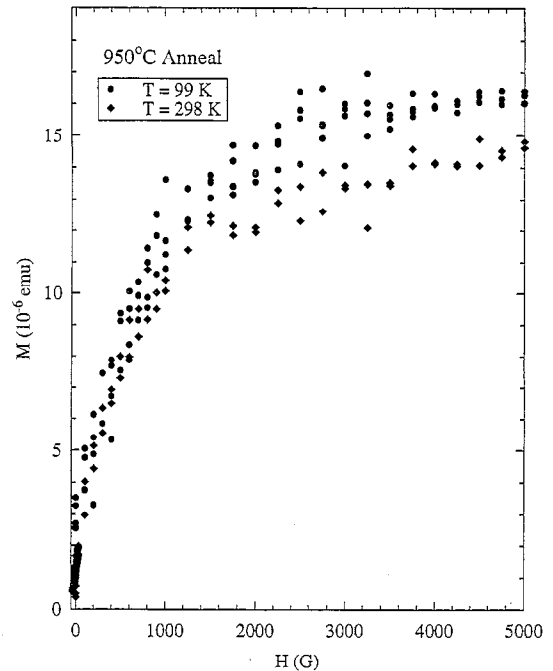


Fig. 4. Magnetization versus field for the  $950^\circ\text{C}$  annealed sample at 99 and 298 K. The magnetization saturates slower than predicted consistent with a multiple domain cluster model. The scatter at high fields is due to the increasing diamagnetic signal.

for clusters larger than  $\sim 10$  nm. The presence of multiple domains in these large clusters would account for the discrepancy between the magnetic behavior and the TEM measurements. Hysteresis measurements were obtained which confirm this. Similar results have been reported for the  $\sim 50$ – $100$  nm Mn-based precipitates [31]. The saturation field we observe would then be a property of the domains. To our knowledge this quantity has not been measured previously for bulk ferromagnetic  $\text{Fe}_3\text{GaAs}$  [25, 26].

In previous work Isaev-Ivanov et al. have measured a static susceptibility  $\chi \cong 10^{-2}$  on melt-grown GaAs with 1–1.5% Fe [25] but did not report a value for the saturation field. To compare with their work, we estimate an implanted volume of  $\sim 2 \times 10^{-6} \text{ cm}^3$  for our sample. From the observed initial slope shown in Fig. 4, we obtain a susceptibility of  $\sim 1 \times 10^{-2}$ . Given the

uncertainties in our sample volume and in the iron concentration of the sample reported by Isaev-Ivanov et al., the agreement is surprisingly good.

We explored the possibility of hysteretic behavior at 300 K for fields between  $\pm 300$  G in the 950°C annealed sample which could occur for multiple-domain clusters. The magnetization displayed a small reproducible hysteresis with a total splitting of 70 G and maximum magnetization of 27% of the saturated value. However, part of this is due to the remanent fields present in our magnet. Measurements of the remanent field at the same temperature and field range used in these hysteresis traces were made using a Hall probe which show a splitting up to 18 G. This sets a lower limit on the coercive field of 25 G. Similar measurements were made at 300 K for fields between  $\pm 1$  T in which the magnetization saturated. This provides an upper limit of 80 G on the coercive field. This indicates bulk  $\text{Fe}_3\text{GaAs}$  is a relatively soft material with a coercive field of  $25 < H_c < 80$  G.

The magnetization behavior of the superparamagnetic clusters is a key scaling parameter for quantitatively describing the behavior of the granular GMR systems. The magnitude of GMR depends on  $\langle \cos \theta_{ij} \rangle$  where  $\theta_{ij}$  is the relative angle between the moments of two successive magnetic scattering particles. In the limit where the orientation of consecutive magnetic particles are uncorrelated,  $\langle \cos \theta_{ij} \rangle = \langle \cos \theta_i \rangle^2 = (M/M_s)^2$  where  $\theta_i$  is the angle between a cluster and the applied field,  $M$  and  $M_s$  are the measured and saturation magnetization of the sample, respectively. Except very near saturation, the GMR contribution to the resistance is found to be well described by  $\rho_m[1 - A(M/M_s)^2]$  where  $\rho_m$  gives the overall magnitude and  $A$  is determined experimentally [18].

Particle size, mean free path ( $A$ ), saturation field, and coercive field have also been shown to be important in previous GMR systems consisting of granular ferromagnetic particles in a metallic host [5, 17–19]. It is believed that an electron must undergo multiple scattering events with different magnetic particles within a single mean free path for large GMR effects to be observed. Optimum particle sizes of a few nm were found in the metallic systems [7]. Clusters much smaller than this are

undesirable since the saturation field scales as  $1/r^3$ . On the other hand, for a fixed magnetic atom concentration, clusters much larger than this have interparticle spacings greater than  $\Lambda$ , reducing the number of scattering events that occur. Our work demonstrates that appropriate sized magnetic particles can be obtained in a semiconductor with moderate annealing temperatures.

The saturation fields we have observed for our  $\text{Fe}_3\text{GaAs}$  samples are comparable with those found in the metallic systems [5, 17, 18]. Further work is required on conducting samples to determine the magnitude of  $\rho_m$  and  $A$  in these materials. The samples we fabricated were non-conducting due to the presence of Schottky-barriers at the semiconductor-cluster boundary which depleted the carriers similar to that observed in GaAs with As precipitates [36]. Doping of the  $\text{Fe}_3\text{GaAs}$  system studied in this work or Fe-implanted InGaAs provide possible routes to a conducting material.

### 3.2. Cluster blocking transition

To study the interactions between clusters we also measured the magnetization as a function of temperature. Zero-field-cooled (ZFC) and field-cooled (FC) data were taken which revealed a blocking transition in all three samples which is evident in Figs. 5–7. For noninteracting clusters we expect a Curie behavior where the magnetization behaves as  $1/T$ . As can be seen, the clusters exhibit a blocking transition. The cusp in each of these figures indicates the transition from a state (well above the cusp) where the thermal energy is large enough to enable the clusters to interact with an external field to a state (well below the cusp) where the thermal energy is no longer able to overcome blocking barriers. This happens for blocking temperatures  $T_b$  of approximately 290, 35, and 3.8 K for the 950°C, 675°C, and unannealed samples, respectively. Similar measurements on the Co–Cu system also show blocking transitions [7, 17]. Two possible sources of the blocking barriers are interactions between neighboring clusters and anisotropy barriers in individual clusters.

If we calculate the variation in blocking temperature as a function of cluster diameter and separation within a model in which superparamagnetic

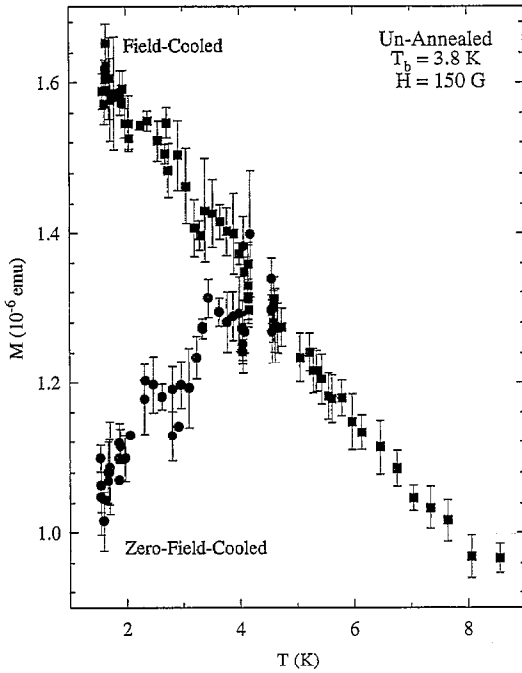


Fig. 5. Zero-field-cooled and field-cooled magnetization versus temperature in a 150 G field for the unannealed sample. The cusp where the ZFC and FC data come together indicates a spin blocking temperature of  $\sim 3.8$  K. The temperature range between 4.15 and 4.60 K is inaccessible in our CCL magnetometer.

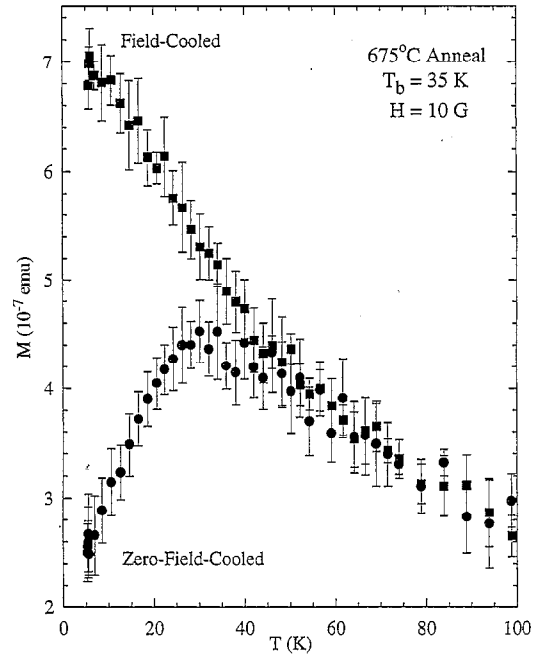


Fig. 6. Zero-field-cooled and field-cooled magnetization versus temperature in a 10 G field for the 675°C annealed sample. The cusp where the ZFC and FC data come together indicates a spin blocking temperature of  $\sim 35$  K.

clusters are coupled through the dipolar interaction, then the force  $F$  between dipoles scales as  $\mu^2/R^3$  where  $\mu$  is the moment of each cluster and  $R$  is the distance between clusters. For a spherical cluster, the moment  $\mu$  would scale as  $r^3$  where  $r$  is the radius of the cluster. Using the particle distributions obtained from our magnetization and TEM data, we find mean particle radii of 14, 2.2, and 0.75 nm for the 950°C, 675°C, and unannealed samples, respectively. However, since the clusters form in a thin layer  $\sim 90$  nm thick, peaked at 85 nm below the GaAs surface, it is not clear whether their distribution is in the two or three dimensional limit.

In a three dimensional model, there would be a density  $\rho_{3D}$  of clusters. If we assume a close-packing, we have  $\rho_{3D} = \frac{4}{3}\pi r^3 / (\sqrt{2}R)^3$ . Thus  $\rho_{3D}$  is proportional to  $r/R$ , or, since  $\rho_{3D}$  is a constant determined by the ion implantation,  $R$  is proportional to  $r$ . Therefore, the dipolar interaction,  $F$ , is

proportional to  $r^3$ . Since the blocking temperature should be proportional to  $F$ , we expect that  $T_b$  is also proportional to  $r^3$ . Similarly, in a two dimensional model in which  $\rho_{2D}$  scales as  $r^3/R^2$ , we would expect that  $F$  and hence  $T_b$  should scale as  $r^{1.5}$ .

Shown in Fig. 8a is a log-log plot of  $T_b$  vs.  $r$ . The number of particles within each of the three samples at a particular radius is shown (in arbitrary units) versus  $r$  in Fig. 8b is shown by the dotted, solid, and dashed lines for the 950°C, 675°C, and unannealed samples, respectively. The distribution for the 675°C and unannealed samples are taken from the fit to the magnetization versus field data while the distribution for the 950°C annealed sample is taken from the TEM measurements. Shown as a solid triangles, circles, and squares, the mean particle radius for the distributions are 14, 2.2, and 0.75 nm for the 950°C, 675°C, and unannealed samples, respectively.

Care must be taken when interpreting the data in Fig. 8. First, the TEM results on the 950°C

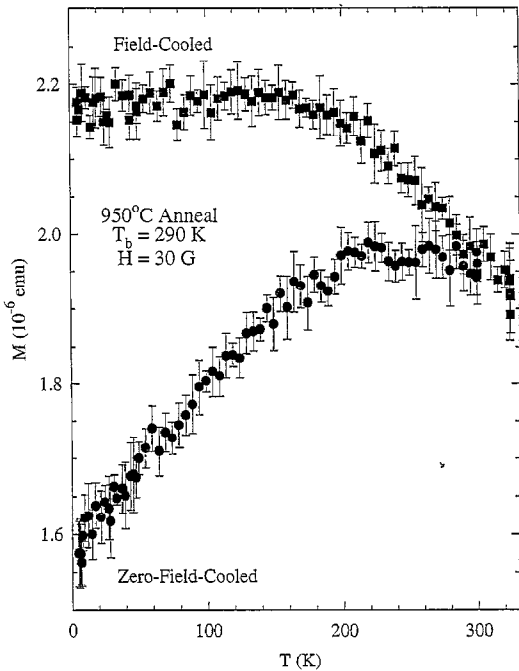


Fig. 7. Zero-field-cooled and field-cooled magnetization versus temperature in a 30 G field for the 950°C annealed sample. The cusp where the ZFC and FC data come together indicates a spin blocking temperature of  $\sim 290$  K.

annealed sample show inter-particle distances of about 100 nm. Since the majority of particles occur in a layer only  $\sim 90$  nm thick, it is reasonable to expect this sample to exhibit a lower blocking temperature as predicted for a two-dimensional distribution. Furthermore, the existence of domains within each cluster of the 950°C annealed sample would reduce its effective moment, also lowering the blocking temperature. For the 675°C and unannealed samples, multiple domain clusters do not appear to be a concern. Since the inter-particle distance is less for smaller clusters, there is enough room in the particle layer for the precipitates to approach a three-dimensional environment.

The variation in blocking temperature expected for the two- and three-dimensional models are shown as lines in Fig. 8. Interpretation is complicated by the broad distribution in particle sizes. As a rough approximation, the mean particle radius for each sample is shown as a solid triangle, circle,

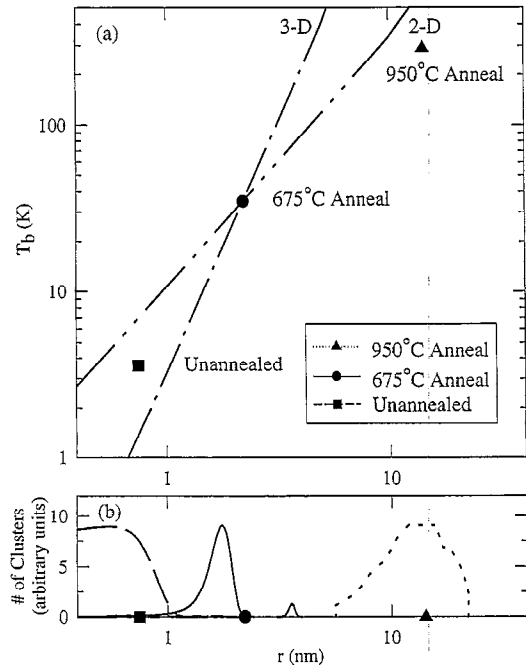


Fig. 8. (a) Blocking temperature versus cluster radius. Predictions for a two- and three-dimensional distribution are shown by the dot-dot-dash and dot-dash lines, respectively. The number of particles at a particular radius is shown in (b) in arbitrary units. The mean radius for the 950°C, 675°C, and unannealed samples is shown as a solid triangle, circle, and square, respectively.

or square in Fig. 8. As can be seen, although both models approximately fit the data, neither model is conclusive. The data are suggestive of a cross-over from two- to three-dimensional behavior.

Alternately, the observed trend in blocking temperature could involve an anisotropy energy barrier in a single isolated cluster which predicts a blocking temperature of  $T_b = KV/25k_B$ , where  $K$  is the anisotropy energy per unit volume,  $V = \frac{4}{3}\pi r^3$  is the volume of the cluster, and  $k_B$  is the Boltzmann constant [37, 38]. This model then predicts that the blocking temperature scales as  $r^3$  which is the same as the three-dimensional dipolar model shown in Fig. 8. If the anisotropy energy is the primary barrier to thermal equilibrium of the moments with the applied field, then the nonpower law behavior observed in Fig. 8 would indicate that the value of  $K$  is not constant. In particular, we



extract  $K = 1.6 \times 10^{-3}$  and  $4.3 \times 10^{-3}$  eV/nm<sup>3</sup> for blocking temperatures of 35 and 3.6 K for the 2.2 and 0.75 nm mean radius clusters, respectively. Since both the anisotropy energy barrier model and the three-dimensional dipolar interaction model scale as  $r^3$ , it is not possible to definitively extract the relative strengths of these two terms from the present data.

#### 4. Conclusion

We have presented magnetization measurements on 1.5, 4.4, and 28 nm mean diameter Fe<sub>3</sub>GaAs clusters located in a layer within 170 nm of the surface of a GaAs wafer. From our measurements, we find that the average cluster has an effective moment of 240, 6000, and 10 000 Bohr magnetons for the 1.5, 4.4, and 28 nm mean diameter clusters, respectively. This demonstrates that the magnetic properties as well as size can be tuned with a post-ion-implant annealing. Fits to the field-dependent magnetization well above the blocking temperature confirm that the 1.5 and 4.4 nm clusters are superparamagnetic which is a key feature of other granular systems which exhibit GMR. Furthermore, the Fe<sub>3</sub>GaAs system shows low saturation fields which are important for applications.

The magnetic and TEM measurements on the 28 nm mean diameter sample are inconsistent with single-domain particles suggesting the presence of multiple domains in these larger clusters. We find a saturation field of  $\sim 2000$  G for temperatures between 100 and 300 K and a hysteresis indicating a coercive field of  $25 < H_c < 80$  G. The saturation and coercive fields observed in these particles provide an estimate for the bulk Fe<sub>3</sub>GaAs system.

Zero-field-cooled and field-cooled measurements reveal a blocking temperature of approximately 290, 35, and 3.8 K for the 28, 4.4, and 1.5 nm mean diameter clusters, respectively. The variation of blocking temperature with interparticle spacing is consistent with either dipolar interactions between clusters or an anisotropy barrier within a single cluster.

With the addition of heavy doping, the potential for a semiconducting GMR material will be ex-

plored. If GMR can be demonstrated in these materials, this work will allow us to tune the magnetic properties to optimize the material for device applications.

#### Acknowledgements

The authors wish to thank J.M. McKenna for his work in thinning the samples. This work was supported by the National Science Foundation (NSF) under Material Research Group Grant No. DMR-9221390 and MRSEC award No. DMR-9400415, and by the US Air Force Office of Scientific Research under grants No. F49620-93-1-0031 and F49620-93-1-0388. One of the authors, T.M. Pekarek, would also like to thank the Purdue Research Foundation for their support.

#### References

- [1] B.J. Hickey, M.A. Howson, S.O. Musa and N. Wiser, *Phys. Rev. B* 51 (1995) 2003.
- [2] E.A.M. van Alphen and W.J.M. de Jonge, *Phys. Rev. B* 51 (1995) 8182.
- [3] J.Q. Wang and G. Xiao, *Phys. Rev. B* 51 (1995) 5863.
- [4] H. Takeda, N. Kataoka, K. Fukamichi and Y. Shimada, *Jpn. J. Appl. Phys.* 33 (1994) L102.
- [5] C.L. Chien, J.Q. Xiao and J.S. Jiang, *J. Appl. Phys.* 73 (1993) 5309.
- [6] S. Zhang and P.M. Levy, *J. Appl. Phys.* 73 (1993) 5315.
- [7] A.E. Berkowitz, J.R. Mitchell, M.J. Carey, A.P. Young, R. Rao, A. Starr, S. Zhang, F.E. Spada, F.T. Parker, A. Hutten and G. Thomas, *J. Appl. Phys.* 73 (1993) 5320.
- [8] M.N. Baibich, J.M. Broto, A. Fert, F.N.V. Dau, F. Petroff, P. Eitenne, G. Creuzet, A. Friederich and J. Chazelas, *Phys. Rev. Lett.* 61 (1988) 2472.
- [9] E.E. Fullerton, D.M. Kelly, J. Guimpel, I.K. Schuller and Y. Bruynseraede, *Phys. Rev. Lett.* 68 (1992) 859 and references therein.
- [10] S.S.P. Parkin, R. Bhadra and K.P. Roche, *Phys. Rev. Lett.* 66 (1991) 2152.
- [11] S.S.P. Parkin, N. More and K.P. Roche, *Phys. Rev. Lett.* 64 (1990) 2304.
- [12] P. Bruno and C. Chappert, *Phys. Rev. Lett.* 67 (1991) 1602.
- [13] W.P. Pratt, Jr., S.F. Lee, J.M. Slaughter, R. Loloee, P.A. Schroeder and J. Bass, *Phys. Rev. Lett.* 66 (1991) 3060.
- [14] M. Jimbo, S. Hirano, K. Meguro, S. Tsunashima and S. Uchiyama, *Jpn. J. Appl. Phys.* 33 (1994) L850.
- [15] J.M. Gallego, D. Lederman, T.J. Moran and I.K. Schuller, *Appl. Phys. Lett.* 64 (1994) 2590.

- [16] R. Schad, C.D. Potter, P. Beliën, G. Verbanck, V.V. Moshchalkov and Y. Bruynseraede, *Appl. Phys. Lett.* 64 (1994) 3500.
- [17] A. Berkowitz, J.R. Mitchell, M.J. Carey, A.P. Young, S. Zhang, F.E. Spada, F.T. Parker, A. Hutten and G. Thomas, *Phys. Rev. Lett.* 3745 (1992) 68.
- [18] J.Q. Xiao, J.S. Jiang and C.L. Chien, *Phys. Rev. Lett.* 3749 (1992) 68.
- [19] J.Q. Xiao, J.S. Jiang and C.L. Chien, *Phys. Rev. B* 46 (1992) 9266.
- [20] F.W. Smith, H.W. Le, V. Diadiuk, M.A. Hollis, A.R. Calawa, S. Gupta, M. Frankel, D.R. Dykaar, G.A. Mourou and T.Y. Hsiang, *Appl. Phys. Lett.* 54 (1991) 890.
- [21] A.C. Warren, N. Katzenellenbogen, D. Grischkowsky, J.M. Woodall, M.R. Melloch and N. Otsuka, *Appl. Phys. Lett.* 58 (1991) 1512.
- [22] D.D. Nolte, M.R. Melloch, J.M. Woodall and S.E. Ralph, *Appl. Phys. Lett.* 62 (1991) 1356.
- [23] D.D. Nolte, *J. Appl. Phys.* 76 (1994) 3740.
- [24] J.C.P. Chang, N. Otsuka, E.S. Harmon, M.R. Melloch and J.M. Woodall, *Appl. Phys. Lett.* 65 (1994) 2801.
- [25] V.V. Isaev-Ivanov, N.M. Kolchanova, V.F. Masterov, D.N. Nasledov and G.N. Talalakin, *Sov. Phys. Semiconductors* 7 (1973) 299.
- [26] I.R. Harris, N.A. Smith, B. Cockayne and W.R. MacEwan, *J. Crystal Growth* 82 (1987) 450.
- [27] H. Ohno, H. Munekata, T. Penney, S. von Molnár and L.L. Chang, *Phys. Rev. Lett.* 68 (1992) 2664.
- [28] H. Munekata, H. Ohno, S. von Molnár, A. Segmüller, L.L. Chang and L. Esaki, *Phys. Rev. Lett.* 63 (1989) 1849.
- [29] M. Tanaka, J.P. Harbison, J. DeBoeck, T. Sands, B. Phillips and T.L. Cheeks, *Appl. Phys. Lett.* 62 (1993) 1565.
- [30] J.M. Kikkawa, J.J. Baumberg, D.D. Awschalom, D. Leonard and P.M. Petroff, *Phys. Rev. B* 50 (1994) 2003.
- [31] J. Shi, J.M. Kikkawa, D.D. Awschalom and P.M. Petroff, *Bull. Am. Phys. Soc.* 40 (1995) 751.
- [32] W. Ostwald, *Z. Phys. Chem.* 37 (1901) 385.
- [33] P.M. Shand, A.D. Christianson, T.M. Pekarek, I. Miotkowski and B.C. Crooker, *J. Appl. Phys.* 79 (1996) 6164.
- [34] A. Mauger, J. Ferre and P. Beauvillain, *Phys. Rev. B* 40 (1989) 862.
- [35] S. Geschwind, A.T. Ogielski, G. Devlin, J. Hegarty and P. Bridenbaugh, *J. Appl. Phys.* 63 (1988) 3291.
- [36] M.R. Melloch, J.M. Woodall, E.S. Harmon, N. Otsuka, F.H. Pollak, D.D. Nolte, R.M. Feenstra and M.A. Lutz, *Annu. Rev. Mater. Sci.* 25 (1995) 547; *Annu. Rev. Inc.* (1995).
- [37] C.P. Bean and J.D. Livingston, *J. Appl. Phys.* 30 (1959) 120S.
- [38] J.F. Gregg, S.M. Thompson, S.J. Dawson, K. Ounadjela, C.R. Staddon, J. Hamman, C. Fermon, G. Saux and K. O'Grady, *Phys. Rev. B* 49 (1994) 1064.